Electrochemical Behavior of Ni-based Alloys as Negative Electrode for Nickel-Metal Hydride Batteries

Liliana Vazquez-Mota[a], Karina Patlán-Olmedo[a], Miguel Angel Oliver-Tolentino[b], Rosa Gonzalez-Huerta[a], Hector Javier Dorantes-Rosales[c], Arturo Manzo-Robledo[a*]

[a] ESIQIE-IPN, Departamento de Ingeniería Química - Laboratorio de Electroquímica y Corrosión. Edif. Z-5 3er piso, UPALM, México D.F. 07738, México.
[b] UPIBI-IPN, Departamento de Ciencias Básicas. Av. Acueducto s/n, Barrio La Laguna, Col. Ticomán, México, D.F. 07340, México.
[c] ESIQIE-IPN, Departamento de Ingeniería en Metalurgia y Materiales. UPALM, UPALM, México D.F. 07738, Mexico.
*amanzor@ipn.mx

Abstract

Nickel-based alloys ($Ni_{0.8}CoO_{0.1}Zn_{0.05}MnO_{0.02}Ti_{0.01}Y_{0.01}Al_{0.01}$ (M1), $NiO_{0.8}CoO_{0.1}Zn_{0.05}MnO_{0.02}Ti_{0.01}Y_{0.01}Al_{0.01}$ (M2) and $NiO_{0.6}CoO_{0.35}Zn_{0.025}Ti_{0.025}$ (M3)) were synthesized from high purity powders by means of high-energy mechanical milling. The hydrogen evolution reaction (HER) kinetic-performance of the as-prepared materials was evaluated using linear sweep voltammetry at alkaline conditions and room temperature. According to kinetic parameters calculated from Tafel slopes, the major activity for the HER was obtained in the sample M2. These results suggest that the surface state in the material play an important role in the proton-adsorption kinetic as demonstrated by SEM, open circuit potential transients and cyclic voltammetry techniques.

1. Introducción

In recent years, nickel-hydride batteries have been widely used as a power source for portable electrical appliances as well as for hybrid low-emission vehicles because of their high-energy density and cleanliness [1,2]. In this context, compared to the rare earth system, hydrogen storage alloys being currently employed as negative electrode materials. In electrochemistry at the electrode surface, a lower exchange current density leads to a higher overpotential. A larger overpotential leads to a decrease in usable capacity and an increase in anode corrosion, and thus results in a further decrease in cycle life. Iwakura et al [3-5] have found that the high-rate discharge ability increases asymptotically with increasing exchange current density. The magnitude of the exchange current density is mainly determined by the structure of the electrodes

and the composition of the hydrogen-absorbing alloys [6], but also by the charge transfer process at the interface between the metal hydride (MH) electrode and the electrolyte. The exchange current density can also be used to derive apparent activation energy, which is a useful intrinsic parameter for evaluating the electrochemical properties of MH electrodes.

In the Ni-MH materials occur charge and discharge reactions where the hydrogen is absorbed, according to equation (1).

$$M + H_2O + e^- \underset{\text{Discharge}}{\overset{\text{Charge}}{\rightleftharpoons}} MH_{abs} + OH^- \qquad (1)$$

This reaction is associated with the Volmer reaction, where, the Hydrogen Evolution Reaction (HER) starts with the proton discharge. In this work the electrochemical behavior of Ni-based alloys in the HER is evaluated as a possible material for negative electrode in the nickel-metal hydride batteries.

2. Experimental Section

2.1 Synthesis of Materials

In this work different materials such as $Ni_{0.8}CoO_{0.1}Zn_{0.05}MnO_{0.02}Ti_{0.01}Y_{0.01}Al_{0.01}$, $NiO_{0.8}CoO_{0.1}Zn_{0.05}MnO_{0.02}Ti_{0.01}Y_{0.01}Al_{0.01}$ and $NiO_{0.6}CoO_{0.35}Zn_{0.025}Ti_{0.025}$ labeled as M1, M2 and M3 respectively were obtained from high-energy mechanical milling. The raw materials were mixed in the appropriate weight ratio to obtain Ni alloys. A total amount of 7 g of the powder mixtures and 6 hardened steel balls of 12.7 mm in diameter were loaded into a steel vial; the mechanical alloying process was carried out at room temperature in an air atmosphere using a shaker mixer/mill machine. The ball-to-powder weight ratio was 7:1. To prevent excessive overheating of the vials, all experiments were carried out by means of cycles of 60 min of milling and 15 min of rest. The milling time tested was 5 h.

2.2 Working Electrode Preparation

The Ni-W alloys were deposited on the previously polished surface (5 mm diameter) of the glassy carbon substrate (GC). The inks were prepared using 5 mg of alloys, 6 µL Nafion (5wt %, Aldrich) and 60 mL of ethanol. The suspension was homogenized by ultrasound. Sample deposits

onto the GC substrate were done with an aliquot of 5 µL of the ink, and then dried in atmosphere of argon for 5 min.

2.3 Scanning Electron Microscopy and EDS analysis

The morphologies of the milling powders were analyzed using a scanning electron microscope, JEOL JSM-6300, working at 15 kV.

2.4 Electrochemical Measurements

A three-electrode standard electrochemical cell was employed. A carbon rod and a Calomel (SCE) electrode were used as counter and reference electrodes, respectively. Prior to use, the solution was purged with argon for at least 15 min. The i-E characteristics were recorded in the interval from -0.1V to 0.4V/SCE. The initial potential was fixed at open circuit potential toward cathodic direction. Solution 5 M of NaOH was used as supporting electrolyte. The electrochemical experiments were done with a Potentiostat/Galvanostat (VersaSTAT 3-200).

3. Result and Discussion

3.1 SEM micrographs

SEM micrographs of Ni based alloys up to 4000X are shown in Figure 1. As can be observed, the samples M1 and M3 with a particle size ranging from 1 to 5 µm, did not presented a well-defined morphology. However, the SEM image for M2 sample (Figure 1-B) show a well defined and uniform particle size in the range of 1µm with agglomerate formation up to 10µm. The EDS analysis (figure not shown) demonstrated the presence of nickel as a main element in the alloys. Some traces of iron were found due to the ball-mechanical milling process.

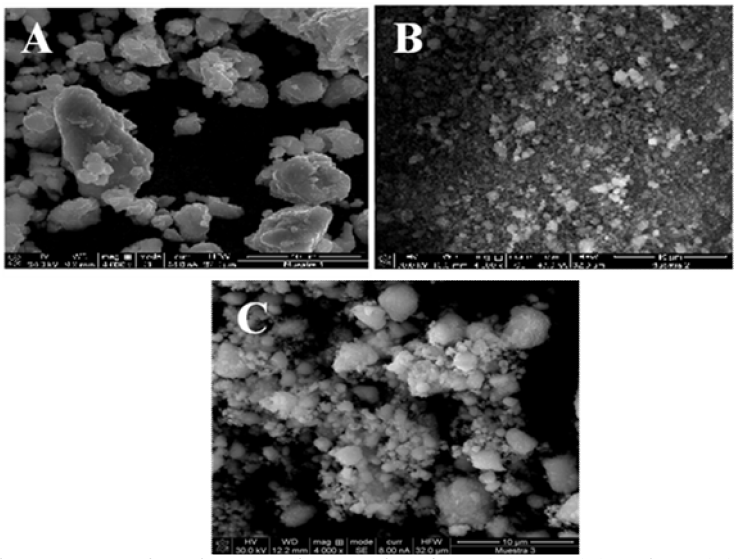

Figure 1. Scanning electron micrographs of M1 (A), M2 (B) and M3 (C).

3.2 Electrochemical measurement

3.2.1 Open Circuit Potential

The open circuit potential (E_{OCP}) is a measurement without a current flow through the external circuit of the electrochemical cell. This technique is sensitive and effective for observing spontaneous phenomena at zero current occurring at the electrode/solution interface.

The E_{OCP} evolution of Ni-based alloys was monitored during 900s (Figure 2) after immersion in a 5 M NaOH solution. These profiles were compared with the signal obtained at the carbon substrate, curve (a) in Figure 2. The E_{OCP} is more positive than the reversible potential for the HER, and also than that corresponding the thermodynamic potential related to the oxidation of Ni to NiO (i.e. E_{rev} =-1.16V); indicating that, at the experimental conditions described here, the Ni-based alloy in turn is covered by a oxide film [7,8] protecting the electrode against further dissolution (corrosion).

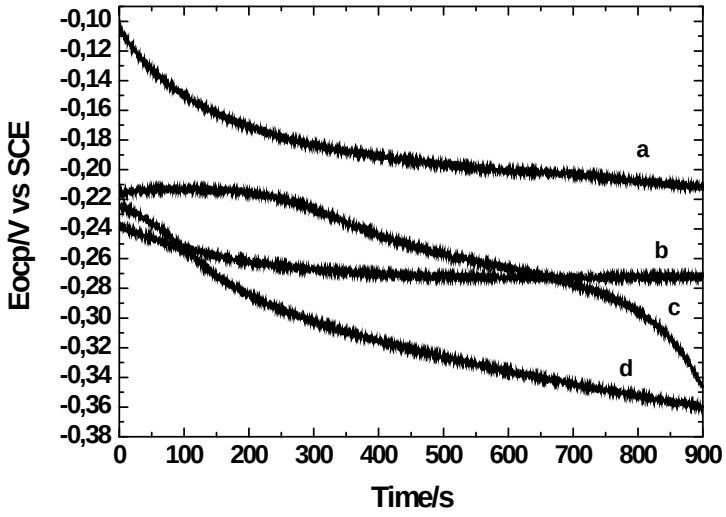

Figura 2. E_{OCP} evolution with the immersion time in 5M NaOH of a) Vulcan, b) M1, c) M2, d) M3.

3.2.2 Cyclic voltammetry

Profiles i-E using cyclic voltammetry (CV) were obtained for the synthesized alloys M1, M2 and M3 in a wide potential window including oxygen- and hydrogen-evolution region. Figure 3 shows the CV of nanocrystalline Ni-based alloys powders as recorded after several cycles, from OCP toward cathodic direction at scan rate of $20mVs^{-1}$. The solution was 0.1M NaOH at 25 ºC. It is interesting to observe that all samples present an anodic peak attributed to the oxidation of Ni(II) to Ni(III) at c.a. 0.35V/SCE [9]. Furthermore, the corresponding reduction peak of Ni(III) is evident at 0.2V/SCE. Notice that in sample M1 (curve a) a cathodic process was found at -0.8V/SCE that can be assigned to the formation of α-$Ni(OH)_2$ [10]. On the other hand, the inset in Figure 3 illustrates the voltammetric profiles obtained at different inversion potentials (E_λ). At these conditions, the profile corresponding to sample M3 did not show redox process for Ni(III)/Ni(II) in the interval from E_λ= -0.4 and -0.6V/SCE. However, when the inversion potential is more negative the current magnitude increases for all cases. These variations are

associated with the adsorption of hydrogen during the negative-going scan, linked to the surface state in the electrode material.

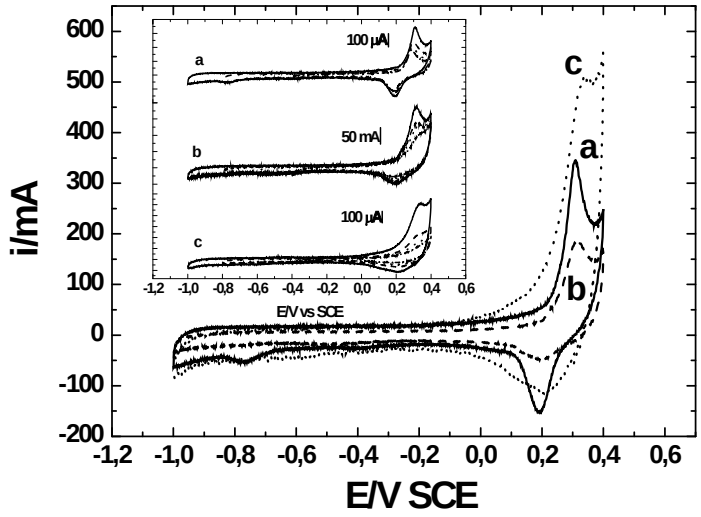

Figure 3. i-E Characteristics of a) M1, b) M2, and c) M3. Inset: Cyclic Voltammetry to different inversion potential.

3.2.3 Electrocatalytic Activity in the HER

Linear polarization profiles of Ni-based alloys, in a solution of 5M NaOH and at scan rate of 5mV/s, are depicted in Figure 4. The production of hydrogen started at -1.2V/SCE for samples M1 (curve a) and M2 (curve b). Conversely, the HER kinetic is lower for sample M3 and carbon Vulcan, see curves (c) and (d), respectively. Typical Tafel plots for the HER at milled metallic powders [11] are shown in the inset. Two Tafel zones are notable for samples M1 and M2 (i) at low overpotentials (from -1200 to -1350 mV/SCE) defined by a slope b1 (mV decade^{-1}); and (ii) at high overpotential regions (from -1350 to -1500 mV/SCE) with a slope defined as b2. However, in sample M3 the Tafel slopes are situated at different region in the i-E profile: b1 in the range -1200 to -1450 mV; and b2 at -1450 to -1500 mV/SCE.

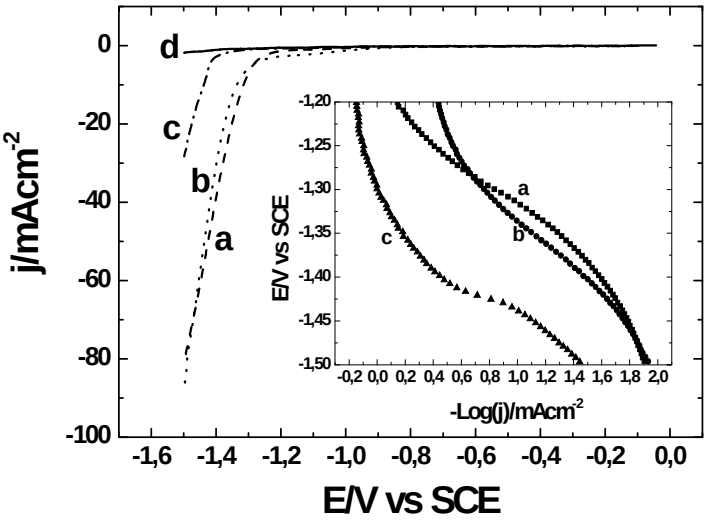

Figure 4. Linear Polarization of a) M1, b) M2, c) M3 and d) Vulcan. Inset: Tafel Plot

Electrokinetic parameters, obtained for the inset in Figure 4, are listed in Table 1. Exchange current densities increase in the order M2>M1>M3. These results indicate that the better electrocatalytic performance can be associated to M2. The differences between tafel plot can be associated to interaction of carbon Vulcan with Ni-base material.

Table 1. Kinetics Parameters

	Tafel slope/mVdecade^{-1}		Log j_o/ mAcm^{-2}
	b1	b2	
M1	91,81	38,16	-6,32
M2	34,47	51,54	-3,52
M3	28,59	80,87	-8.28

4. Conclusion

The electrocatalytic activity of Ni-based materials obtained by mechanical alloying was evaluated in the hydrogen evolution reaction (HER) at alkaline conditions. The SEM analysis showed that the presence of Y and Al induce particle size ranging from 1 to 5μm, repressing the

formation of agglomerates. OCP transients and CV techniques give some clues concerning the surface state in the alloys. Kinetic parameters in the HER region were determined using linear polarization. The alloy $NiO_{0.8}CoO_{0.1}Zn_{0.05}MnO_{0.02}Ti_{0.01}Y_{0.01}Al_{0.01}$ (M2) was found to yield the highest intrinsic electrocatalytic activity versus hydrogen production.

Acknowledgements
Project ICyTDF-PICS08-29 for financial support.

References

1. T. Sakai, T. Hazama, H. Miyamura, N. Kuriyama, A. Kato, H.Ishikawa, J. Less-Common Met. 172-174 (1991) 1175.
2. F. Feng, D.O. Northwood, Surf. Coatings Tech. 167 (2003) 263.
3. C. Iwakura, M. Matsuoka, K. Asai, T. Kohno, J. Power Sources 38 (1992) 335.
4. M. Matsuoka, K. Asai, Y. Fukumoto, C. Iwakura, J. Alloys Comp. 192 (1993) 149.
5. C. Iwakura, Y. Fukumoto, M. Matsuoka, T. Kohno, K. Shinmou, J. Alloys Comp. 192 (1993) 152.ç
6. H. Kronberger, Int. J. Hydrogen Energ. 21 (1996) 577.
7. M. Metikos-Hukovic, Z. Grubac, N. Radic, A. Tonejc, J. Mol. Catal. A-Chem 249 (2006) 172.
8. A. Królikowski, E. Plonska, A. Ostrowski, M. Donten, Z. Stojek, J. Solid State Electrochem. 13 (2009) 263.
9. N.V. Krstajic, V.D. Jovic, Lj. Gajic-Krstajic, B.M. Jovic, A.L. Antozzi, G.N. Martelli, Int. J. Hydrogen Energy 33 (2008) 3676.
10. H. Chi-Chang, C. Chen-Yi, J. Power Sources 111 (2002) 137.
11. K. Lian, D.W. Kirk, S. Thorpe, Electrochim. Acta 36 (1991) 537.